Summer 2022

An Innovative Elastohydrodynamic Seal Concept for Gases

Matthew J. DeMond

AN INNOVATIVE ELASTOHYDRODYNAMIC SEAL CONCEPT FOR GASES

by

MATTHEW DEMOND

(Under the Direction of Sevki Cesmeci)

ABSTRACT

Supercritical CO_2 (sCO_2) power cycles are next generation power technologies offering improved efficiency, lower customer costs, and less water usage. They hold significant potential in many different industries such as nuclear power production, ship propulsion, geothermal power, solar power, and fossil fuel power plants. One of the largest hurdles preventing this milestone is the lack of suitable shaft seals for sCO_2 operating conditions. This component issue needs to be addressed for the next generation nuclear turbine and compressor development to progress. In this study, a novel Elastohydrodynamic (EHD) seal is proposed. This proposed design is capable of handling high pressure and high temperature while being a scalable shaft seal for sCO_2 turbomachinery. The potential benefit of this design includes low leakage, minimal wear, low cost, and no stress concentration. The focus of this study was to perform a proof-of-concept study utilizing physics-based computer simulations. A Fluid-Structure-Interaction (FSI) modeling approach was utilized, and the simulations were carried out in COMSOL Multiphysics software. The results indicated that the proof-of-concept study was successfully demonstrated. The leakage rate obtained from the physics-based computer simulations followed a quadratic form with a peak at $\dot{m}$ = 0.075 kg/s at P_{in} = 15 MPa and then decaying to less than $\dot{m}$ = 0.040 kg/s at P_{in} = 30 MPa. This trend signifies that the design has the potential to be optimized and be tailored to be a solution to the shaft sealing issues found during the operation of sCO_2 turbomachinery.

INDEX WORDS: Seal, Supercritical carbon dioxide, sCO_2, Turbomachinery, Power plant, Power cycles, CFD, FSI

AN INNOVATIVE ELASTOHYDRODYNAMIC SEAL CONCEPT FOR GASES

by

MATTHEW DEMOND

B.S., Georgia Southern University, 2020

A Thesis Submitted to the Graduate Faculty of Georgia Southern University

in Partial Fulfillment of the Requirements for the Degree

MASTER OF SCIENCE

ALLEN E. PAULSON COLLEGE OF ENGINEERING AND COMPUTING

AN INNOVATIVE ELASTOHYDRODYNAMIC SEAL CONCEPT FOR GASES

by

MATTHEW DEMOND

Major Professor:	Sevki Cesmeci
Committee:	Prakashbhai Bhoi
	Hayri Sezer

Electronic Version Approved:
July 2022

DEDICATION

I would like to dedicate this work to my family and friends who have supported me throughout this journey.

ACKNOWLEDGMENTS

I would like acknowledge Dr. Sevki Cesmeci for his continual support throughout my undergraduate and graduate careers at Georgia Southern. I also want to acknowledge my lab mates Fuad Hassan and Rubayet Hassan for their assistance. I would like to thank my committee members Dr. Prakashbhai Bhoi and Dr. Hayri Sezer for their time and guidance.

TABLE OF CONTENTS

Page

LIST OF TABLES

Page

LIST OF FIGURES

Page

NOMENCLATURE

sCO_2	Supercritical CO_2
EHD	Elasto-hydrodynamic
CFD	Computational Fluid Dynamics
FEA	Finite Element Analysis
FSI	Fluid-Structure Interaction
RANS	Reynolds-averaged Navier–Stokes

CHAPTER 1

INTRODUCTION

Background

The production of efficient, cost effective and environmentally friendly power is an issue that effects everyone on the planet. Since the industrial revolution, many different methods of generating electricity have been explored. Many of these methods rely on fossil fuels to generate heat which is then converted to electricity. These methods have developed over the years from various forms of the steam engine to high performance internal combustion engines. While these methods of power generation have helped to develop much of the technology that we use and see today, they have also had a negative impact on the environment. With the mass adoption and use of fossil fuels, the emission of greenhouse gasses has led to global warming and environmental pollution (White et al. 2021). Due to these negative effects, cleaner more efficient methods of power generation must be developed to keep up with the ever-increasing demand. Renewable technologies such as wind and geothermal are being actively developed to generate sustainable power. Unfortunately, this technology has not developed rapidly enough to keep up with the power demand from society. However, having diverse means of power generation is required as society progresses. This sparked the development of nuclear power, solar power, hydrogen and other efficient thermodynamic power cycles (Ahn et al. 2015).

Power generation methods that utilize these thermodynamic power cycles will likely continue to be the bases of future energy solutions. However, the traditional open Brayton cycles or indirect-fired, closed Rankine cycles are no longer efficient enough. Different working fluids, such as supercritical CO_2, are being explored to determine their impact on the efficiency of the power cycles. Supercritical CO_2 power cycle have been found to be a promising candidate due to

having thermal efficiencies greater than 50%, low water and fuel usage, small physical footprint, and lower capital costs which result in lower overall electricity costs. The thermal efficiency when compared to other power conversion techniques can be seen below in Figure 1. Research and development of this technology has gained significant traction over the past 10 years as this power cycle technology gets applied to nuclear, geothermal, solar and other thermodynamic cycles (White et al. 2021).

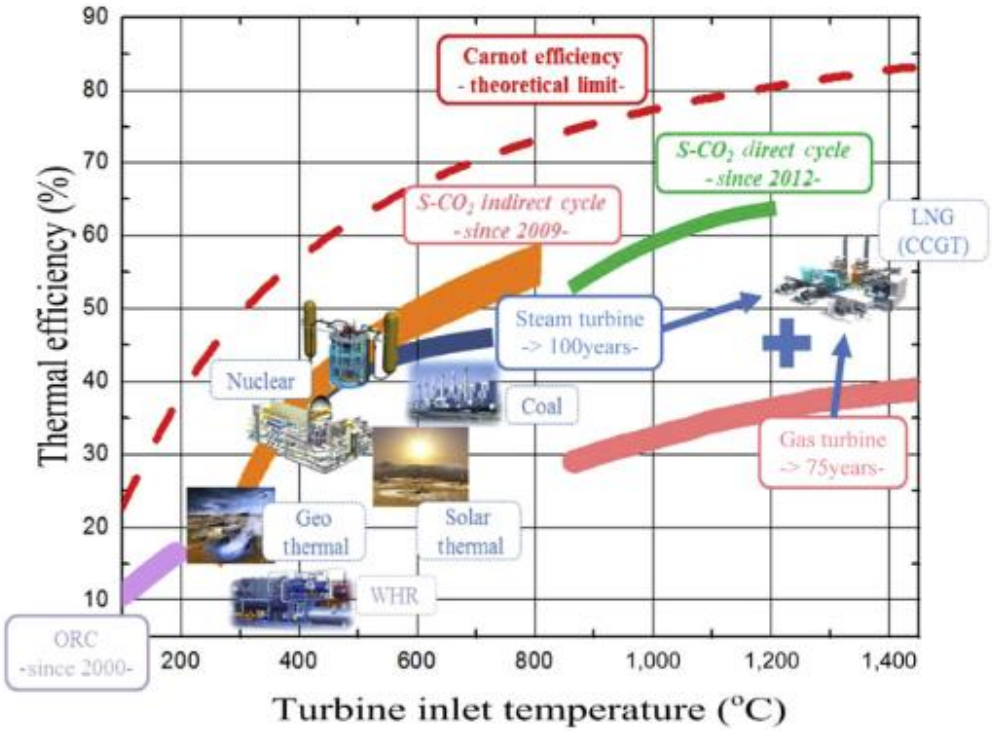

Figure 1: Thermal Efficiency Comparison of Power Conversion Systems (Ahn et al. 2015)

Problem Statement

Due to the high temperature and pressures encountered when using supercritical CO_2 as the working fluid, shaft end seals are a major concern for the realization of this new technology. While small scale turbines rated for 0.3-10MW are not impacted by this issue, large, utility scale turbines

rated for >100MW will suffer the most. In a recent study, a 450MW turbine utilizing a labyrinth seal has an efficiency loss of approximately 0.55% to 0.65% on a 51.9% scale due to leakage past the seal. This corresponds to millions of dollars lost per cycle due to lack of efficiency and cost to replenish the lost CO_2 (Bidkar et al. 2017). There have been other seal designs that have been proposed to be utilized in this technology. These seals include various labyrinth seal designs, brush seals, compliant foil seals and finger seals.

Each seal design has their own disadvantages that would negatively impact the overall efficiency of the supercritical CO_2 power cycle. First, the labyrinth seal currently being utilized in the 450MW turbine is known to have a high leakage rate. Due to the operating condition and working fluid, brush seals encounter significant bristle wear. Compliant foil seals have scalability issues that limit their use in utility scale turbines. Lastly, the complexity of finger seals inhibits their implantation into this technology. The development of an innovative, low leakage non-contact seal design is critical to unlock the full potential of supercritical CO_2 power cycles.

Hypothesis

If an innovative new seal can leverage the proven elastohydrodynamic (EHD) lubrication sealing mechanism to reduce CO_2 leakage, then this design will offer a high pressure, low leakage, scalable sealing solution needed for the full realization of supercritical CO_2 power cycles and other turbomachinery.

CHAPTER 2

LITERATURE REVIEW

Turbomachinery

Turbomachinery has two main categories in mechanical engineering. These categories are turbines and compressors or pumps. These components each have two requirements which are a rotor and a working fluid. In a turbine, energy is transferred from the fluid to the rotor. In the case of a turbine on an aircraft, fuel is burned, and the expansion of the ignited gas causes the rotor to turn. In a compressor, the rotor is powered, and energy is transferred from the rotating shaft to the working fluid. Turbines and compressors can range in size from a few centimeters to several meters in diameter. No matter the size, the working fluid fulfills such a critical role in efficient and reliable function of turbomachinery. For either system, controlling the interface clearances is critical to manage the working fluid. Due to cost, manufacturability, and working parameters of the systems, tight tolerances between components is not a feasible means of sealing the working fluid within the system. Additional sealing solutions must be designed and implemented to maintain high operating efficiencies of turbines, compressors, and pumps without negatively effecting the performance of the system (Chupp et al. 2006).

A variety of designs and materials can be used to create a seal for turbomachinery. Each seal design and material have advantages and disadvantages that must be considered. The seal designs can be catered to the size, working conditions, pressure, temperature, rotor speed, and many other factors that make each turbomachine different. The seal designs for turbomachinery can be broken down into two main categories, contact and non-contact seals. Contact seals make physical contact with the rotor to seal in the working fluid. Non-contact seals either never contact

the rotor or only make contact on startup of the system. This seal design is generally ideal for low maintenance, low cost, and low wear applications (Chupp et al. 2006).

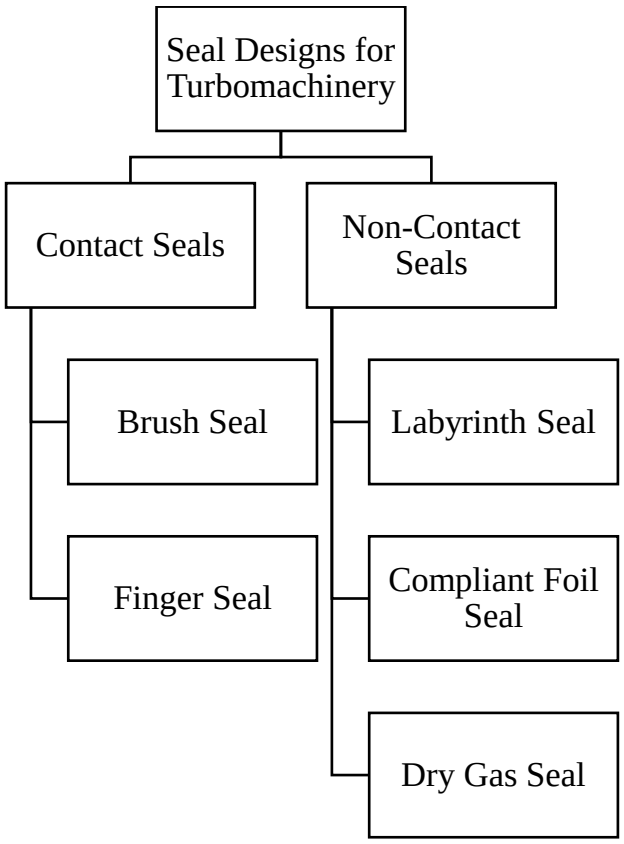

Figure 2: Seal Designs for Turbomachinery

Supercritical CO_2 power cycles is one application for these innovative new seal designs. Since this system's efficiency is affected heavily by seal leakage and wear, this application is the driving force for many new seal designs entering the market today.

Supercritical CO_2 Power Cycles

The production of efficient, cost effective, and environmentally friendly power is an issue that effects everyone on the planet. After the industrial revolution, the world relied mostly on fossil fuels to generate electricity. As technologies began to advance, the demand for the electricity also

increased leading to increases in pollution and greenhouse gas emissions (White et al. 2021). Supercritical CO_2 power cycles offer several benefits over traditional power generation techniques. This power cycle uses supercritical CO_2 as the working fluid. This working fluid is ideal due to its density and viscosity values. The density of the fluid remains high which closely resembles properties of its liquid state, while maintaining the viscosity of its gaseous state (Kim et al. 2019). This results in benefits including high efficiency, small component size, and low cost (Kulhánek and Dostál 2011). This type of power generation has grown substantially over the past decade due to a major increase in investments to develop this technology (White et al. 2021).

One of the major limiting factors that has prevented this technology from seeing even higher efficiency numbers are the current shaft end seals (Bennett et al. 2019). Some of the current sealing solutions that are utilized in this method of power generation are labyrinth seals, dry gas seals, compliant foil seals, and finger seals. Labyrinth seals are considered to be the more conventional seal design. Dry gas seals are also used in larger supercritical CO_2 power cycles. Due to the complexity of the seal, labyrinth seals are still more likely to be selected for this specific application (Kim et al. 2019). Other advanced contact seals like finger and brush seals were also developed for this application. Each seal design has merits in both efficiency and production cost depending on the application. More recently non-contact seals like film riding seals and hydrodynamic seals are being developed to further decrease leakage past the seal and improve efficiency. Non-contact seals have been found to offer less leakage and longer life since they are not in contact with the rotor like finger and brush seal designs. Researchers are currently working towards creating a non-contact seal that can be used in supercritical CO_2 power cycles and other high pressure turbomachinery applications (Bidkar et al. 2017). To help unlock the full potential

of supercritical CO_2 power cycles, innovative seal designs must continue to be developed to improve both efficiency and lifespan of the seal.

The hydrodynamic face seal is one of the best candidates for this operating condition due to its ability of withstanding large pressure differentials. These pressure differentials can be as high as 1,000 psia. Currently, large scale hydrodynamic face seals are not commercially available due to both manufacturing and design challenges (Bidkar et al. 2017).

Labyrinth Seals

Labyrinth seals are used in turbomachinery to control leakage between high- and low-pressure zones. These seals can be used in gas, steam, and hydraulic turbines (Pena de Souza Barros et al. 2019). This seal utilizes a set of teeth that face the spinning rotor. Since the seal never contacts the rotor, this seal is considered a non-contact seal. As the gas or fluid travels through the teeth, pressure continually decreases minimizing the overall leakage rate. Due to the nature of the seal design, leakage rates are heavily dependent on the operational parameters of each application. These parameters include pressure, shaft speed, and overall shaft diameter. In general, the leakage rate of this seal is proportional to the gap area and is also inversely proportional to the number of teeth on the seal (Kim et al. 2019). In most cases, leakage decreases by almost 20% in high velocity conditions (Wu and San Andrés 2019). This seal design is currently being used in supercritical CO_2 turbines and is one of the oldest seal designs currently being used for this application. These seals have a loss between 0.55% and 0.65% on thermodynamic cycle efficiency on a 51.9% efficient cycle. This is a considerable amount of loss resulting in a high efficiency penalty for the whole system (Bidkar et al. 2017). Due to this inefficiency, other seal designs are being developed to minimize leakage and further improve the efficiency of the machines they are used on. An example of a labyrinth seal can be seen below in Figure 3.

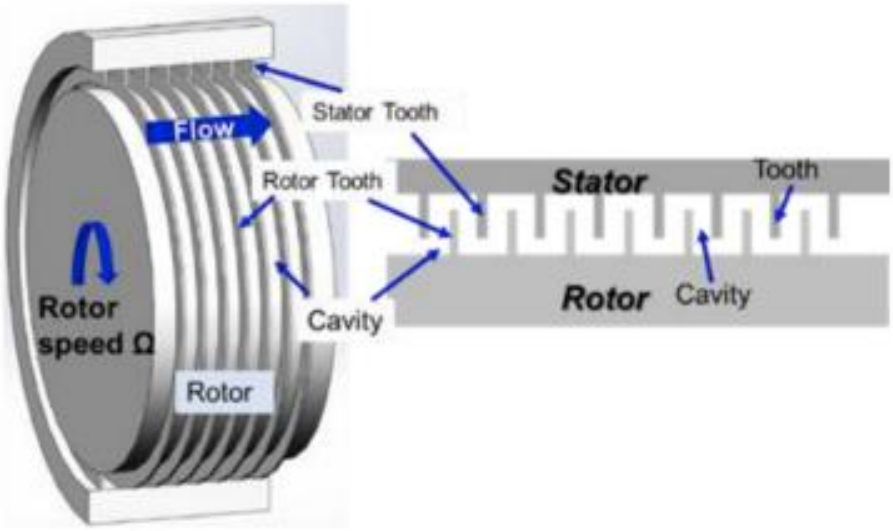

Figure 3: Labyrinth Seal (Wu and San Andrés 2019)

Brush Seals

Brush seals are another common sealing solution used in turbomachinery. These seals consist of brushes that are aligned with a rotor in the tangential direction. These seals allow the rotor to move due to vibration or thermal growth. Due to this property, these seals offer lower leakage rates than labyrinth seals. A backing plate in the axial direction supports the bristles and prevents them from bending in the direction of the spinning rotor (Proestler 2002). This seal design is considered a contact seal as the brushes contact the spinning rotor. Since the seals make contact with the spinning rotor, these seals wear out significantly quicker when compared to non-contact sealing solutions (Bidkar et al. 2017). They also cause wear on the rotor surface. To improve the efficiency of the seal, and to retrofit the design to multiple applications, many different parameters of the seal can be changed. These changes include, bristle thickness, lay angle, bristle length, backing plate gap, and front plate gap. In some applications, multiple brush seals are used to achieve the desired leakage rate (Proestler 2002). An example of a brush seal can be seen below in Figure 4.

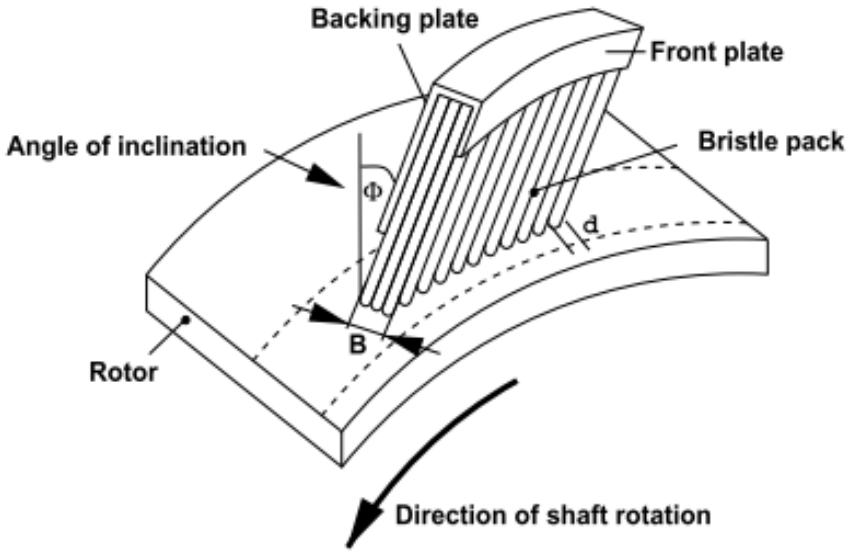

Figure 4: Brush Seal (Proestler 2002)

Compliant Foil Seals

Compliant foil seals offer a similar sealing solution as both labyrinth seals and brush seals. These seals are mostly used in secondary flow systems of aircraft engines (Wang et al. 2020). These seals consist of a seal membrane, a floating seal ring, seal base and several elastic supporting sheets (Hou et al. 2020). An example of a complaint seal can be seen below in Figure 5. The compliant seal can move and adjust to any changes in rotor diameter caused by thermal expansion or vibrations. This movement is due to the elastic supporting sheets. Since the seal never touches the spinning rotor, this seal design is considered a non-contact seal. The life span of the seal is significantly better due to this no contact operating configuration (Heshmat et al. 2013). This design allows leakage to be minimized in the small gaps of secondary flow systems (Hou et al. 2020). There are several reasons why this seal design has not gained traction in the supercritical CO_2 power cycle and turbomachinery application. First, is the perception that this design is only

good for light weight and high-speed rotors. The second is inexperience in foil bearing design which leads to the belief that this design is not robust enough for demanding environments like high loads and temperature. Researchers are currently working to develop this design and change the perception of this sealing solution (Heshmat, Walton II, and Córdova 2018).

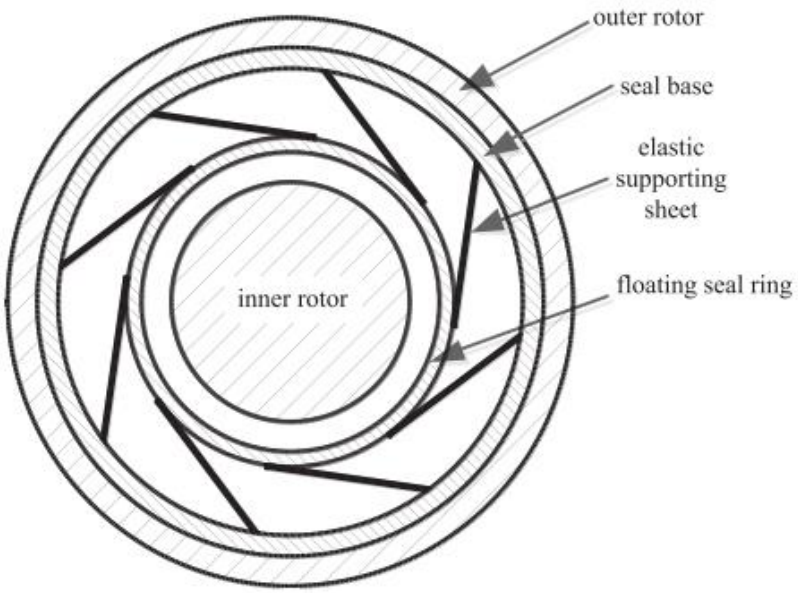

Figure 5: Compliant Seal (Hou et al. 2020)

Finger Seals

Finger seals have a lower manufacturing cost when compared to brush seals. This seal design is also able to better adapt to thermal changes than labyrinth seals. Due to these characteristics, this seal design has been adopted for use in various aero-engine applications (Zhao, Su, and Chen 2020). Like brush seals, finger seals fit into the same category of contact seals. This is because the fingers make contact with the rotor (Bidkar et al. 2017). Over time, this results in the various components of the seal wearing and breaking down. In most cases, the fingers are made from either metal or a carbon/composite. Finger seals are a significant advancement from labyrinth seals as they offer lower leakage rates and higher overall efficiency. It was also found that for

many years during the development of this seal, researchers focused on the leakage through the finger seal radial clearance. The leakage that made it past the finger seal bundles was not being considered when calculating the efficiency of the seal (Zhao, Su, and Chen 2020). This resulted in a lower overall efficiency rating for the seal once all leakage points were considered. Due to all the components in this seal, the complexity is a major downfall of this specific seal design. An example of a finger seal can be seen below in Figure 6.

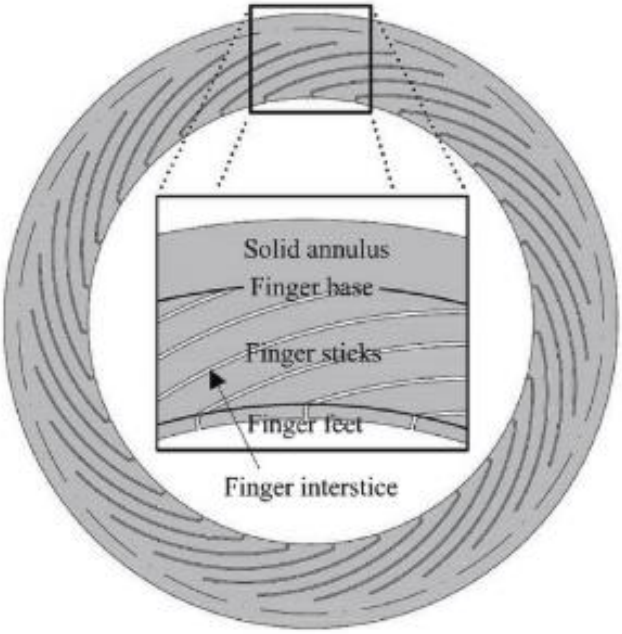

Figure 6: Finger Seal (Zhao, Su, and Chen 2020)

Dry Gas Seals

Dry gas seals have several key benefits over other traditional mechanical sealing systems for turbomachinery (Su, Rahmani, and Rahnejat 2017). This seal design can withstand incredibly high rotational speeds (20,000 RPM to 30,000 RPM) without the aid of a traditional oiling system. They also offer extremely competitive leakage rates when compared to other high performance shaft end seals. Due to the nature of the seal design, dry gas seals are able to work efficiently with

a wide variety of gasses and operating conditions (Rozova and Martynenko 2020). These benefits have caused this seal design to replace traditional oil ring seals in compressors. Dry gas seals can also be run in dual and triple seal configuration when sealing volatile fluid systems. These configurations help to further reduce the leakage of these harmful chemicals in to the environment (Su, Rahmani, and Rahnejat 2017). The multistage design also allows for each stage to be optimized to handle a certain pressure value resulting in an overall more efficient seal. An example of this sealing design can be seen below in Figure 7.

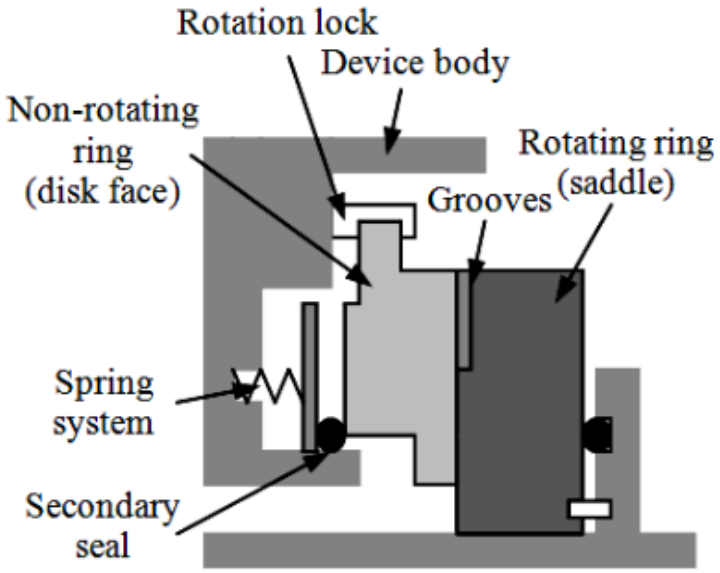

Figure 7: Dry Gas Seal (Rozova and Martynenko 2020)

Elasto-hydrodynamic Lubrication (EHD)

Lubrication is critical to the performance and reliability of any functional mechanical system. Metal on metal contact that is not properly lubricated can have detrimental effects on the lifespan and efficiency of the system. When properly designed, the lubricant film that covers the two contact surfaces provides protection from any excessive wear. The thin fluid layer that coats

the components can withstand high enough pressures to induce significant elastic deformation on the components. This phenomena is known as elastohydrodynamic lubrication (Habchi et al. 2008).

The foundation of this topic dates to 1886 when Osborne Reynolds published a paper discussing the pressure distribution and load carrying compacity of fluid films (Lugt and Morales-Espejel 2011). Elastohydrodynamic (EHD) lubrication, specifically, has made major strides in the last few decades. The first major publication involving this topic specifically was published in the late 1930's. Since then, the study of elastohydrodynamic lubrication has played a critical role when designing a variety of machine components. The components that utilize this phenomena include anything from bearings to gears (Peterson et al. 2020).

Due to the complexity and nature of elastohydrodynamic lubrication, computer modeling and Computational Fluid Dynamics (CFD), are being used to help understand and apply this lubrication technique to many different applications, including single and multistage seals for turbomachinery.

Fluid Solid Interaction (FSI)

Computational Fluid Dynamics (CFD) modeling and Fluid-Solid-Interaction (FSI) analysis are integral steps in the design and development of many systems and components today, including seal design. There are many different companies that offer off-the-shelf CFD software packages. Some of the companies that offer these packages include ADINA, Open FOAM, ANSYS, SOLIDWORKS, and COMSOL Multiphysics.

These software packages each have multiple ways of solving complex problems. These solution methods are segregated or full coupled solver approaches. Segregated solvers solve the

corresponding pressure and velocity equations separately, while utilizing variables from the previous solver iteration. The segregated solving method is generally ideal for incompressible or weakly compressed flows. Fully coupled solvers solve all equations simultaneously. The fully coupled solvers are generally used for highly compressible flows and are able to capture flow details like pressure, energy, and momentum of the flow (Schowalter et al. 2007).

The interaction of fluids and solids can be seen every day. Interactions as simple as the trees moving due to wind is an example of a fluid-solid-interaction (Benra et al. 2011). While simple, computational modeling of this phenomenon has taken many decades to be developed. The EHD lubrication modeling requires both fluid and solid mechanics. FSI software packages are necessary to simulate and solve this style problem (Peterson et al. 2020). The CFD simulations use the full Navier-stokes equations to solve problems that involve EHD lubrication. This is more accurate than the traditional modified Reynolds equations. The Reynolds equation is not appropriate to apply to EHD theory for gases due to its inability to consider highly compressible flow at high pressures.

This study is novel in that a comprehensive design methodology is proposed for an innovative elastohydrodynamic (EHD) seal concept. The seal concept is explored and analyzed using fully coupled FSI simulations carried out in COMSOL Multiphysics software. This specific method of design and analysis has not yet been explored for this style seal design.

CHAPTER 3

METHOD

Overview

The purpose of this study is to develop a sealing system that can offer low leakage rates, low drag, low cost, smoother system startups, and minimal wear. The proposed single EHD seal, shown below, is attached to a back ring and sits on a rotor with cold clearance *h*. The seal is attached directly to the back ring with zero clearance at start when engine pressure P_1 is equal to P_2. After the rotor ramps up, pressure P_1 will be greater than pressure P_2. Due to operating pressure P_1, the EHD seal will deform inwardly and throttle the leaking gas flow. The minimum clearance will never be zero, because this condition will close the leakage path and back the pressures upstream all to P_1, which will re-open the throat. Meanwhile, the leaking gas flow will push the EHD seal open to avoid further wear.

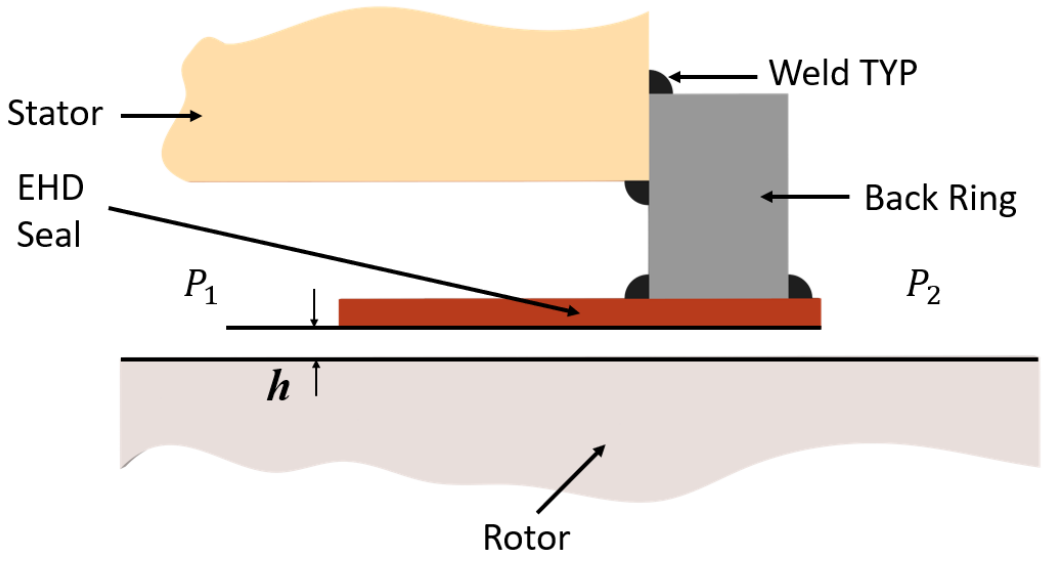

Figure 8: EHD Seal in Cold Condition

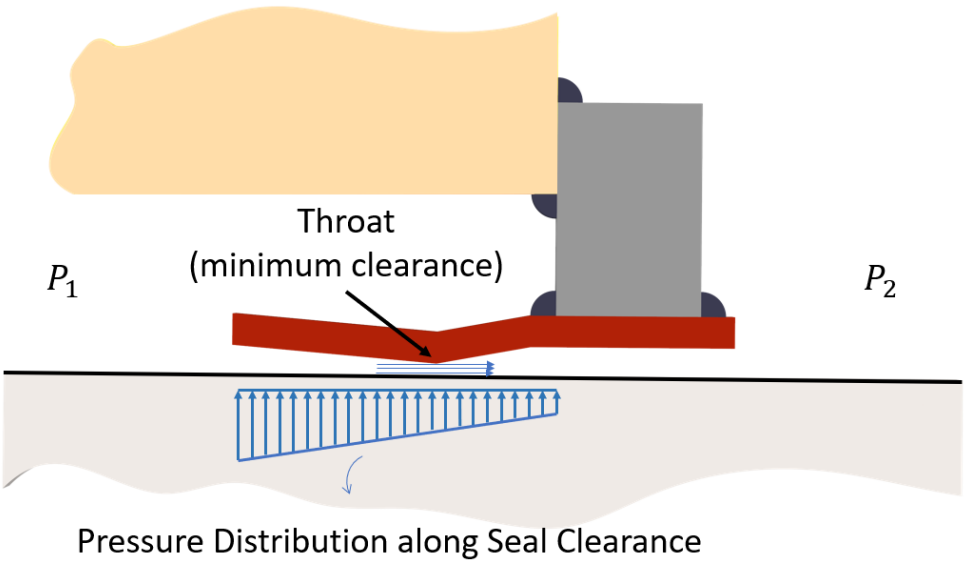

Figure 9: EHD Seal in Operating Condition

Analytical Modeling

The proposed elastohydrodynamic (EHD) seal leverages the proven EHD lubrication theory. In most cases, the EHD lubrication theory is studied using the Reynolds equation. This equation can be seen below in Eq. 1 (Gong et al. 2016).

$$\frac{\partial}{\partial x}\left(\frac{\rho h^3}{\mu}\frac{\partial P}{\partial x}\right)+\frac{\partial}{\partial z}\left(\frac{\rho h^3}{\mu}\frac{\partial P}{\partial x}\right)=6\frac{\partial(\rho u h)}{\partial x}+6\frac{\partial(\rho v H)}{\partial z}+12\frac{d(\rho h)}{\partial t} \quad (1)$$

Unfortunately, this equation, is only valid under a set of strict parameters. The conditions that must be met to utilize this equation are steady, laminar, and incompressible flow. Due to the high-pressure differentials encountered by this proposed sealing solution, the compressible flow will need to be considered when analyzing the system. This makes the Reynolds equation a poor method for analyzing the seal design and performance. Physics-based computer simulations will be the primary mode of analysis as this method utilizes the full Navier-Stoke equations in the solver with turbulence models.

Physics-Based Computer Simulations

Computational fluid dynamics (CFD) modeling is the next available solution that can handle the flow conditions that will be present during the seals' operation. There are many different commercially available simulation software solutions that are capable of handling the Fluid-Solid-Interaction (FSI) found in this sealing system (Figure 10). In this study, COMSOL Multiphysics will be used to carry out all fully coupled FSI simulations.

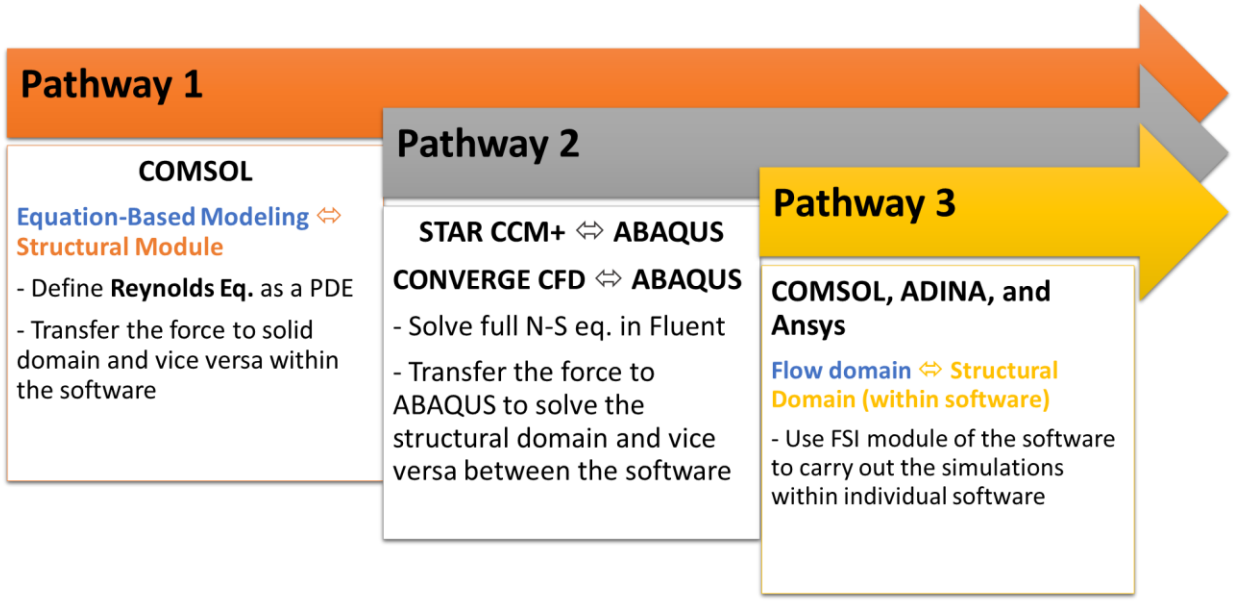

Figure 10: Simulation Process Flow Chart

Verification Study

As a general rule, when carrying out CFD and FEA simulations, simulation methodology must be verified either via comparisons with analytical modeling or experimental study. For the case of this study, the experimental data is not readily available. Thus, comparisons can be made with analytical modeling. To this end, one-way coupled simulations were carried out by using the

famous Reynolds equation, which is a simplified form of Naiver-Stokes equation for flow through narrow passages. The general form of the Reynolds equation in COMSOL is given by

$$\frac{\partial}{\partial x}\left(-\frac{\rho h^3}{12\mu}\frac{\partial P}{\partial x}\right)+\frac{\partial}{\partial y}\left(-\frac{\rho h^3}{12\mu}\frac{\partial P}{\partial y}+\frac{\rho h}{2}(v_a+v_b)\right)=0 \qquad (2)$$

where ρ is the density of the fluid, h is the film thickness (or the height of the clearance), μ is the dynamic viscosity, P is the pressure, v_a is the rotational velocity of the rotor, and v_b is the rotational velocity of the sleeve. In this study, the sleeve was stationary, and the effect of the rotational speed of the rotor was neglected. Hence, the governing Reynolds equation was simplified to

$$\frac{d}{dx}\left(-\frac{\rho h^3}{12\mu}\frac{dP}{dx}\right)=0 \qquad (3)$$

The sleeve was made of structural steel, and carbon dioxide was used as a working fluid. The density and dynamic viscosity of carbon dioxide is a function of pressure and temperature. For the proof-of-concept studies, the density of the carbon dioxide was modeled by using the ideal gas equation, which is given by

$$\rho=\frac{P}{RT} \qquad (4)$$

where R is the gas constant, and T is the working temperature which was considered constant in this study. The viscosity normally is a function of temperature and pressure, but for simplicity, in this work, the viscosity was considered to be a constant. The ideal gas assumption is valid for low-density gasses, when away from the critical point region and the saturated vapor line on P-v curves as known from Thermodynamics. In this study, the working pressures go up to 15 MPa, resulting in high-density carbon dioxide. The errors associated with the use of the ideal gas equation can be mitigated by introducing the compressibility factor to the ideal gas equation. However, this is

beyond the scope of this work and is left for future work. By using the geometric and material properties shown in Table 1, one-way coupled simulations were carried out in COMSOL. In one-way coupled simulations, the flow domain in the clearance is solved, and the pressure data is fed to the solid domain (seal geometry) to determine the deformation of the seal under the influence of pressure at the top and bottom of the seal.

Table 1**:** Geometric and Material Properties (Verification Study)

Material Properties	
Property/Parameter	**Value**
Rotor radius (r_{rotor})	25.4 mm
EHD seal thickness (t_{seal})	0.5 mm
EHD seal length (L_{seal})	26.035 mm
Initial clearance (h_0)	0.05 mm
Dynamic viscosity of CO_2 (μ) @293 K	1.46e-5 Pa-s
Young's modulus of the seal (E)	2e11 N/m^2
Density of CO_2 (ρ)	f(P)
Working pressure (P_0)	Varying
Ambient pressure (P_e)	0 Gauge
Gas constant of CO_2	0.1889 kJ/(kg*K)
Working temperature	293 K

As for the analytical solution, integration of Eq. 3, using the ideal gas equation for density and applying the boundary condition, yields

$$P_{analytical} = \sqrt{P_0^2 + \frac{(P_e^2 - P_0^2)x}{L_{seal}}} \tag{5}$$

where the pressures are in terms of absolute pressure. Hence, the results from the COMSOL and analytical modeling can be compared to verify the simulation methodology. Such comparison is shown in Figure 11 below.

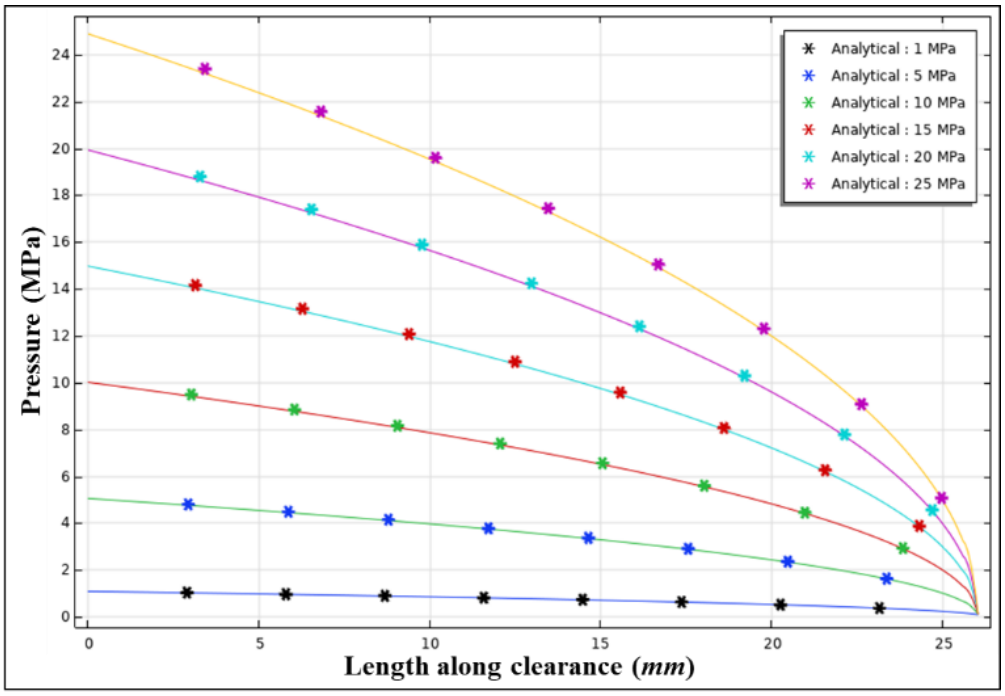

Figure 11: Comparison of the Analytical Solutions with Simulation Data for Pressure Field Using One-Way Coupling

As seen from Figure 11, the results from COMSOL and analytical modeling for the pressure variation in the clearance matched perfectly. Thus, it is concluded that the fully coupled simulations can be performed to study the behavior of the seal under design operating conditions.

Model Setup and Meshing

The seal geometry is critical to the function and performance the EHD seal. The initial geometry that will be used can be seen below in Figure 12. The dimension of the seal design is as follows: $L_{EHD} = 26.035$ mm, $t_{EHD} = 0.5$ mm, $h_{EHD} = 0.05$ mm, $R_{rotor} = 25.4$mm, $R_{housing} = 50.8$ mm.

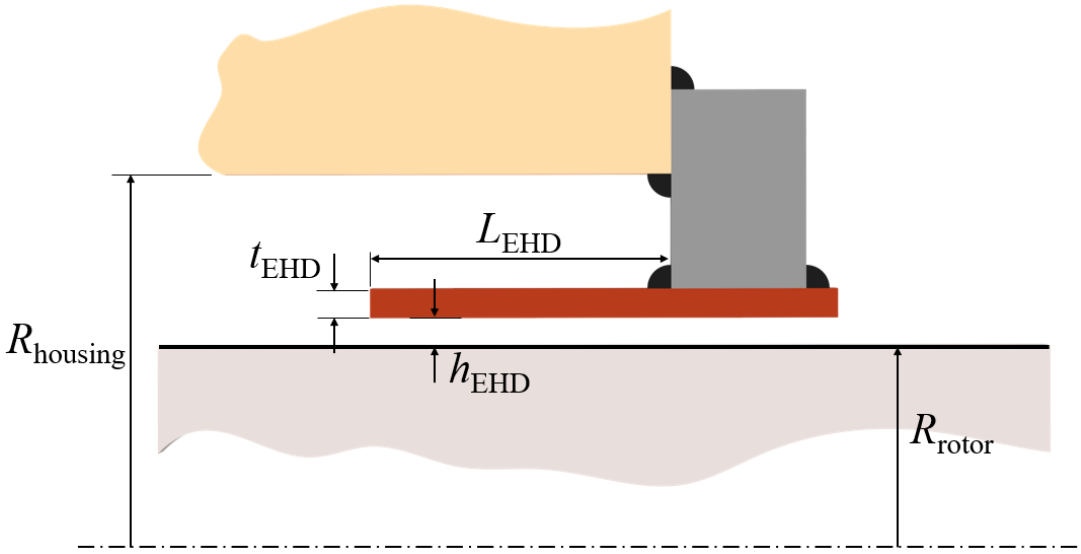

Figure 12: Seal Design Dimensions

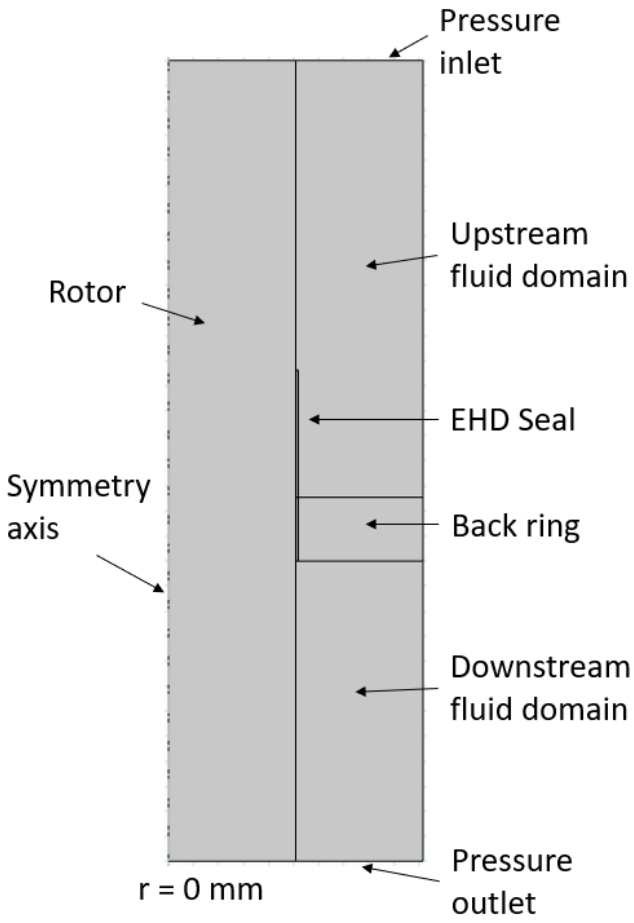

Figure 13: Model with Main Components Labeled

The models were configured to run as efficiently as possible. To aid it both time and computational power efficiency, all simulations were conducted in a 2D axisymmetric model. All model components excluding the clearance between the seal and the rotor were meshed using triangular elements. For higher accuracy, the clearance between the seal and the rotor was meshed using rectangular elements. In combination with the "wall functions" within the solver, all fluid boundaries were assigned boundary layers to capture the highly viscous effects near the walls. In total, the mesh contained 133,471 domain elements and 5,384 boundary elements. The maximum element size within the clearance between the seal and the rotor was set to 0.025mm. The mesh used can be seen in Figures 14(a) and 14(b).

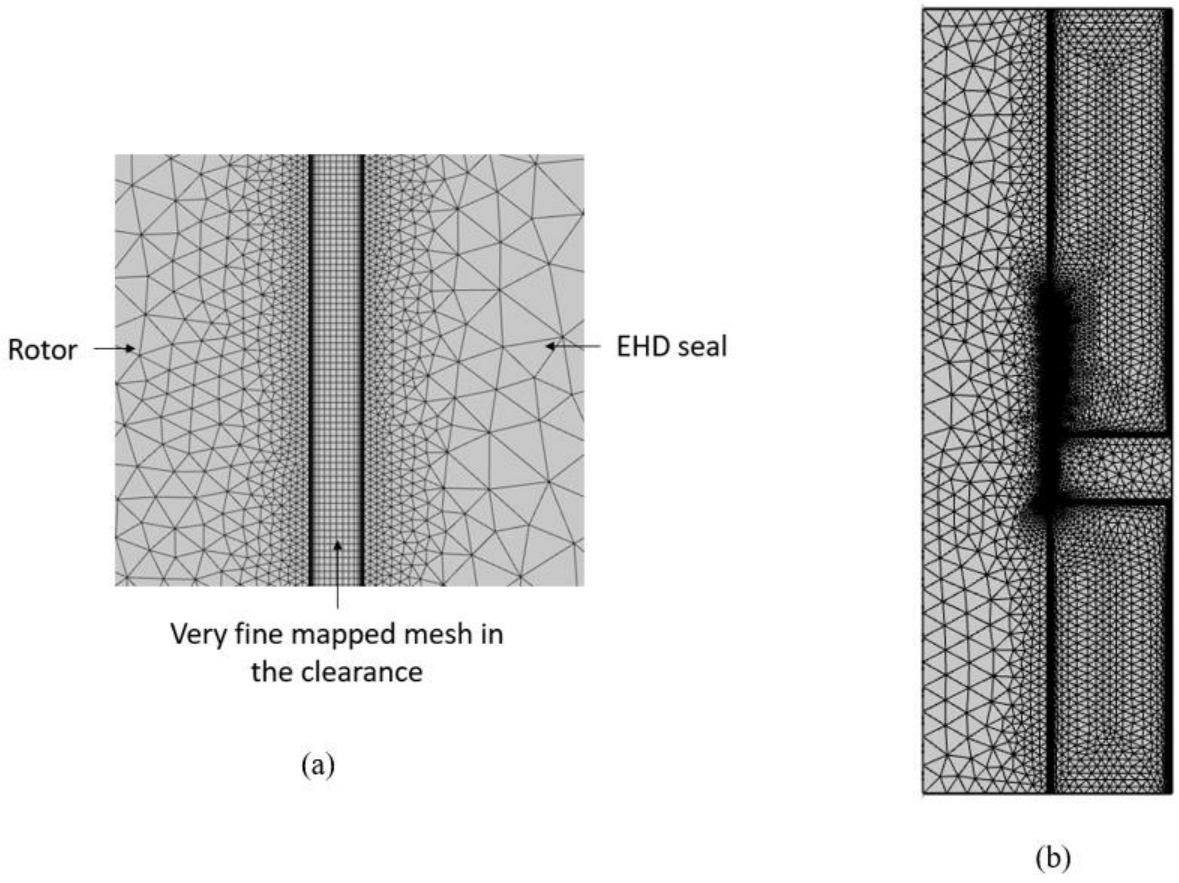

Figure 14: (a) Mesh in the clearance (b) Overall generated Mesh

Materials

In this proof-of-concept study, the solid and fluid components were assigned as structural steel and nitrogen, respectively. The material properties are shown in Table 2.

Table 2: Material Properties

Material Properties	
Gas Type	Nitrogen
Gas Inlet Pressure (Pa)	1.01e5 - 3.5e7
Solid Material Type	Steel
Young's Modulus (Pa)	2.00E+11
Density of Solid (kg/m^3)	7850
Poisson's Ratio of Solid	0.3

The properties of the fluid used in the simulation are defined by several different equations. The density of the nitrogen used is defined by the ideal gas equation, while the dynamic viscosity and thermal conductivity are defined by Sutherland's Law. The equations for dynamic viscosity and thermal conductivity can be seen below.

Thermal conductivity:

$$k = k_{\text{ref}} \left(\frac{T}{T_{k,\text{ref}}} \right)^{3/2} \frac{T_{k,\text{ref}} + S_k}{T + S_k} \tag{6}$$

where T is the temperature, $k_{\text{ref}} = 0.0241\ \text{W/m} \cdot \text{K}$, and $T_{k,\text{ref}} = 273\ \text{K}, S_k = 194\ \text{K}$.

Dynamic viscosity:

$$\mu = \mu_{\text{ref}} \left(\frac{T}{T_{\mu,\text{ref}}} \right)^{3/2} \frac{T_{\mu,\text{ref}} + S_\mu}{T + S_\mu} \tag{7}$$

where μ is the dynamic viscosity, $\mu_{\text{ref}} = 1.716e^{-5}\ \text{Pa} \cdot \text{s}$, and $T_{\mu,\text{ref}} = 273\ \text{K}, S_\mu = 111\ \text{K}$.

Boundary Conditions

The pressure inlet, P_{in}, of the model is varied across the entire operational range of the seal, from 0.1 MPa to approximately 35 MPa. The reference fluid temperature at the inlet is set to 310 K. The pressure outlet was set to standard atmospheric pressure. All fluid solid boundaries are set to solid walls with fixed constraints, excluding the seals geometry. The seal's geometry is left free to deform. All fluid solid boundaries, including the seals geometry, were set as thermal insulation.

It is important to note that the energy equation is only being solved in the fluid domain and that there is no heat transfer between the fluid and solid boundaries. This results in no thermal loading being considered in the solid domain. However, the fluid and solid boundaries are fully coupled through the applied boundary conditions that surrounds the entirety of the seal geometry. This allows the pressure and shear stresses to still be applied to the seals geometry as boundary loads. This ultimately allows the seal to deform.

Computational Method- Fluid Domain

The High Mach Number Flow (HMNF) module within COMSOL Multiphysics was used to account for the compressible and turbulent effects that would likely occur in flow downstream from the seal and near the seals clearance with the rotor. Reynolds-averaged Navier–Stokes (RANS) turbulent model type was selected. The most common turbulence model, k – ϵ, was selected and Kays – Crawford heat transport turbulence model was used. The following equations were used to solve the fluid domain.

Steady continuity:

$$\nabla \cdot (\rho u) = 0 \tag{8}$$

Steady Navier – Stokes:

$$\rho(u \cdot \nabla)u = \nabla \cdot [-pI + K] + F \tag{9}$$

Turbulence model equations:

$$K = (u + \mu_T)(\nabla u + (\nabla u)^T) - \frac{2}{3}(u + u_T)(\nabla \cdot u)I - \frac{2}{3}\rho kI \tag{10}$$

$$\rho(u \cdot \nabla)k = \nabla \cdot \left[\left(\mu + \frac{\mu_T}{\sigma_k}\right)\nabla k\right] + P_k - \rho\epsilon \tag{11}$$

$$\rho(u \cdot \nabla)\epsilon = \nabla \cdot \left[\left(\mu + \frac{\mu_T}{\sigma_\epsilon}\right)\nabla \epsilon\right] + C_{\epsilon 1}\frac{\epsilon}{k}P_k - C_{\epsilon 2}\rho\frac{\epsilon^2}{k}, \quad \epsilon = ep \tag{12}$$

$$\mu_T = \rho C_\mu \frac{k^2}{\epsilon} \tag{13}$$

$$P_k = \mu_T[\nabla u : (\nabla u + (\nabla u)^T) - \frac{2}{3}(\nabla \cdot u)^2] - \frac{2}{3}\rho k \nabla \cdot u \tag{14}$$

Steady Energy equation:

$$\rho C_p u \cdot \nabla T + \nabla \cdot q = Q \tag{15}$$

$$q = -k\nabla T \tag{16}$$

where ∇ is the gradient operator, u is the velocity vector, ρ is the density, τ is the viscous stress tensor, P is the pressure, C_p is the specific heat capacity at constant pressure, F is the volume force vector, q is the heat flux vector, T is the absolute temperature, S is the strain-rate tensor, Q contains the heat sources, k is the thermal conductivity, K is the turbulent kinetic energy, μ is the dynamic viscosity, ep is the turbulent dissipation rate, μ_T is the eddy viscosity, $C_{\epsilon 1}$, $C_{\epsilon 2}$, σ_ϵ, and σ_k are adjustable constants. The dependent variables in the above equations are u (including u, v, w), $p, k, ep,$ and T.

Computational Method- Solid Domain

The following equations were used to solve the solid domain.

$$0 = \nabla \cdot (FS)^T + F_V, \quad F = l + \nabla u2 \tag{17}$$

where, FS (F being the deformation gradient) is the 1st Piola-Kirchhoff stress tensor, l is the unit tensor, u2 is the displacement, F_V is the volume force vector.

CHAPTER 4

RESULTS AND DISCUSSION

In this study, the focus was to validate the proposed seal design using physics-based computer simulations. The first step in analyzing the results is examining the deformation of the seal. The boundary load distribution along the top and bottom of the seal can be seen in Figure 15. The load distribution along the top of the seal was found to be uniform while the load along the bottom of the seal decreased from tip to the root of the seal.

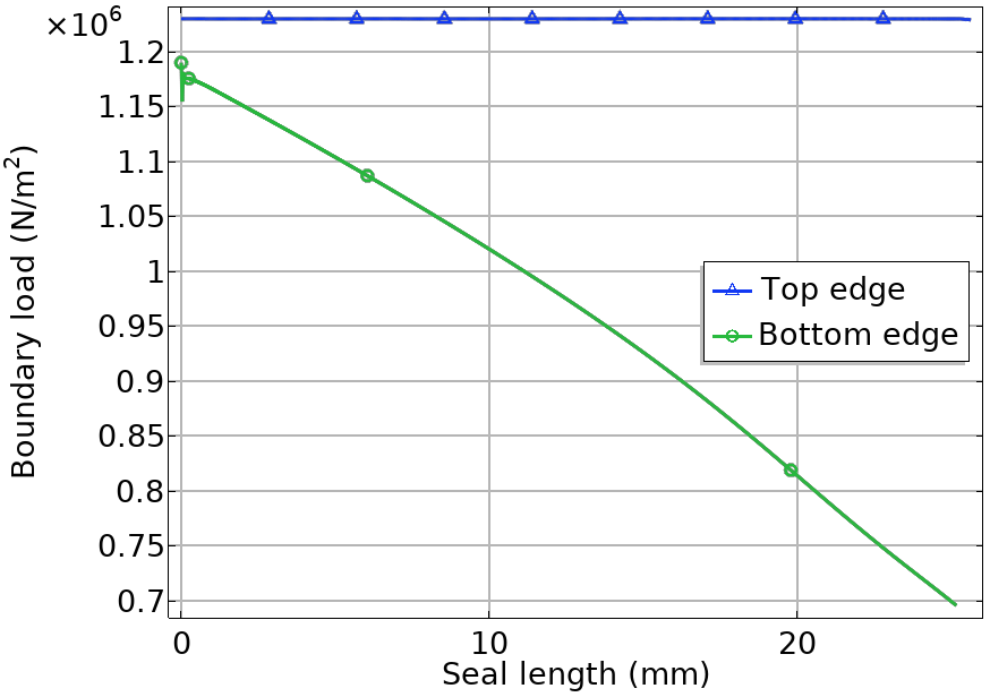

Figure 15: Applied Boundary Loading Along the Top and Bottom of the Seal at P_{in}= 1 MPa

Next, the combined effects of the uniform load along the top of the seal and the gradient along the bottom of the seal results in the deformation of the seal shown in Figure 16. The left end of the graph indicates the tip of the seal, and the right end of the graph represents the root of the

seal. As expected, there is a formation of a throat towards the root of the seal. This is indicated by the corresponding notation on Figure 16.

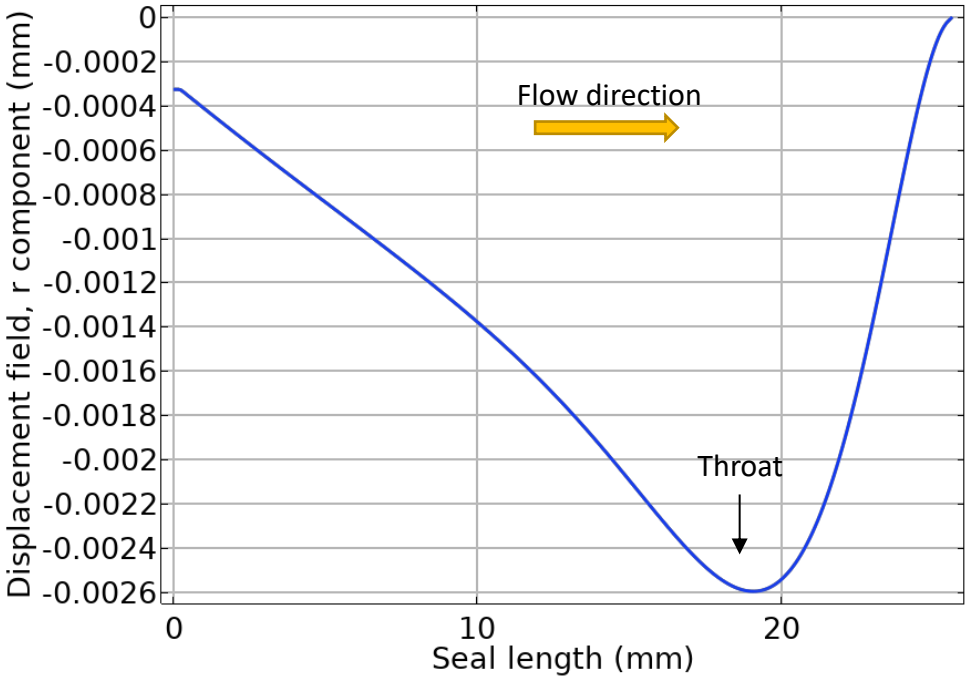

Figure 16: Deformation of the Proposed EHD, Formation of a Throat Labeled, P_{in}= 1 MPa

The 2D displacement field is shown in Figure 17. This allows better visualization of the deformation that occurred to the seal. It is important to note that the maximum deformation of the seal at P_{in}= 1 MPa was found to be 0.0026mm resulting in a throat height of 0.0474mm. The deformation value is expected to increase, and the throat height is expected to decrease as the input pressures rises. As explained previously, the throat height will never be zero. If this were to happen, the pressure differential formed would result in the throat of the seal reopening, allowing gas to flow.

This phenomenon is very challenging to model with modern computer simulations. A minimum predefined gap must be set between the seal and the rotor. This is necessary to avoid

computational issues such as topological problem and mesh failures in the clearance between the seal and the rotor. However, in this study, the simulation was run until the solution yielded convergence errors.

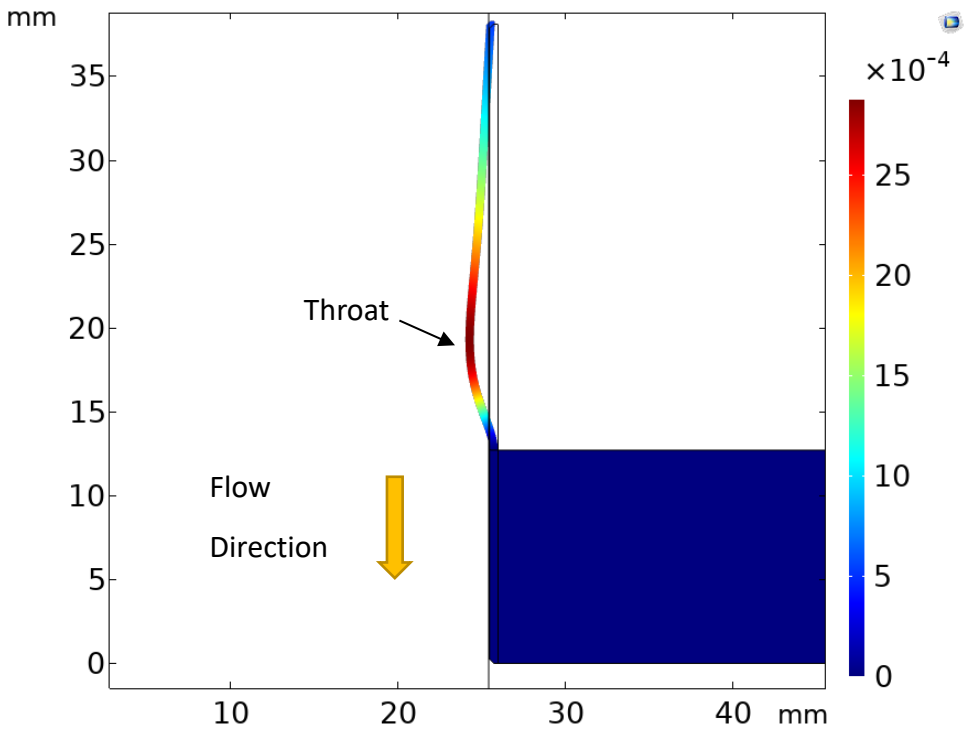

Figure 17: 2D Displacement Field with Throat Formation, Displacement Magnified 50E3%

The simulations were then conducted several times with different input pressures. The pressure ranged from 0.1 MPa to 35 MPa. As expected, the deformation of the seal increased as the input pressure increased. This trend can be seen in Figure 18. The throat began to form close to the root of the seal for all trials. It is important to note that the throat gap at P_{in}= 35 MPa was found to be 2.5 µm.

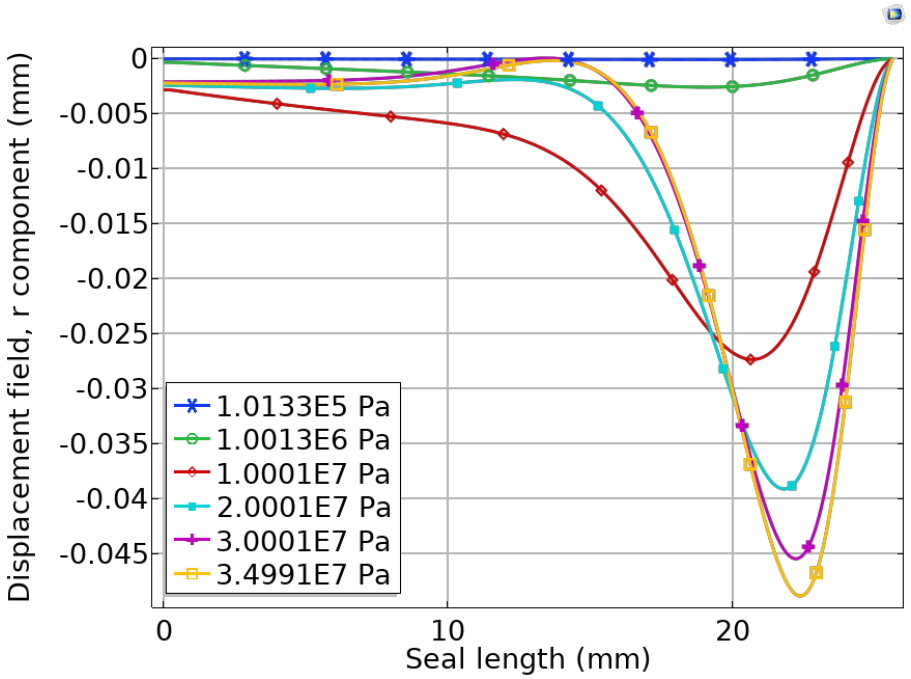

Figure 18: Deformation of the Seal from P_{in} = 0.1 MPa to 35 MPa

It is also important to analyze the material properties of the gas flowing in the clearance between the seal and rotor. The temperature, density, pressure, and dynamic viscosity of the gas flowing in the clearance of the seal were all collected. The data is displayed in Figures 19, 20, 21, and 22, respectively. This data was collected from the bottom boundary of the seal. It is important to note that the data collected in the clearance supports Sutherland's Law and the Ideal gas equation previously discussed.

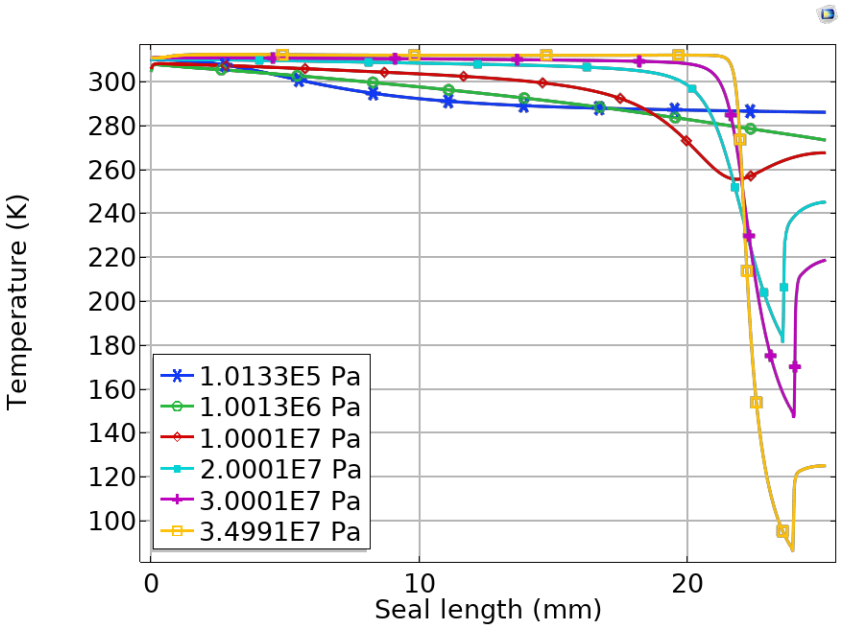

Figure 19: Temperature Data Collected from Bottom Boundary of the Seal

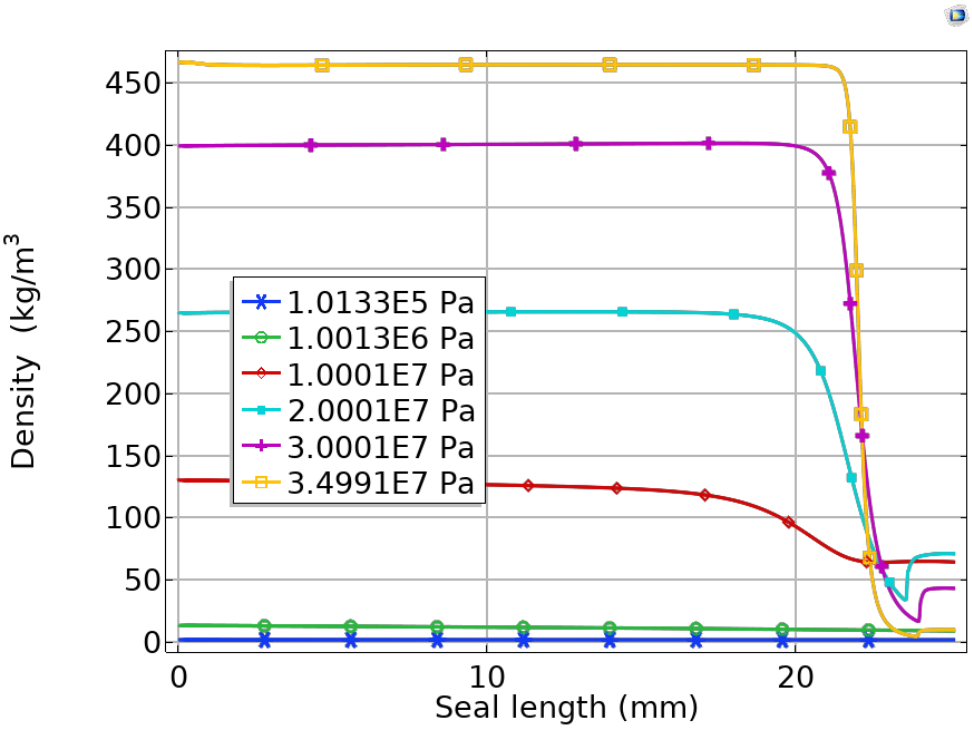

Figure 20: Density Data Collected from Bottom Boundary of the Seal

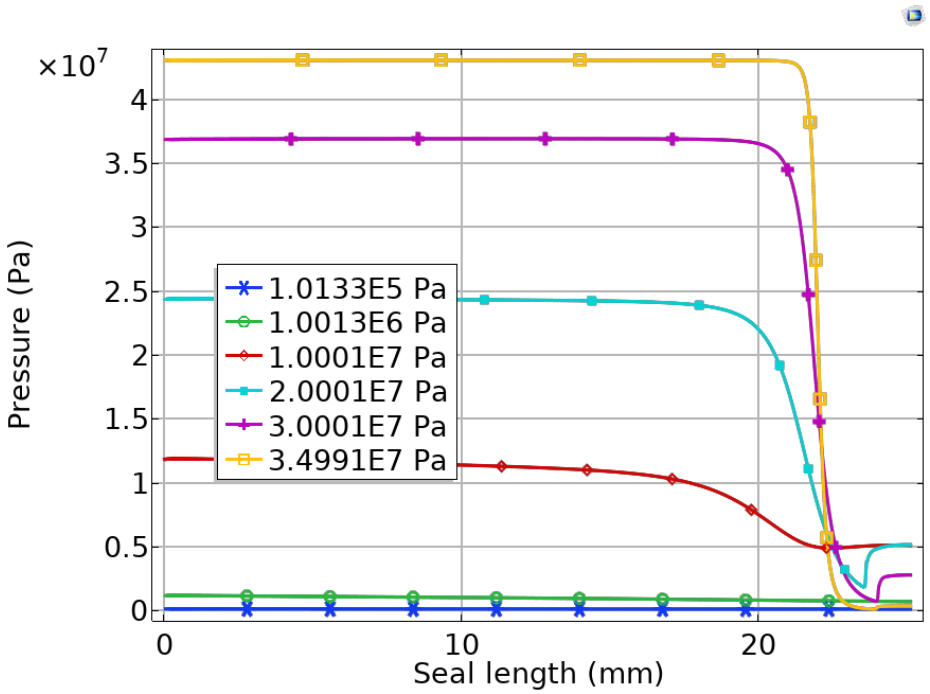

Figure 21: Pressure Data Collected from Bottom Boundary of the Seal

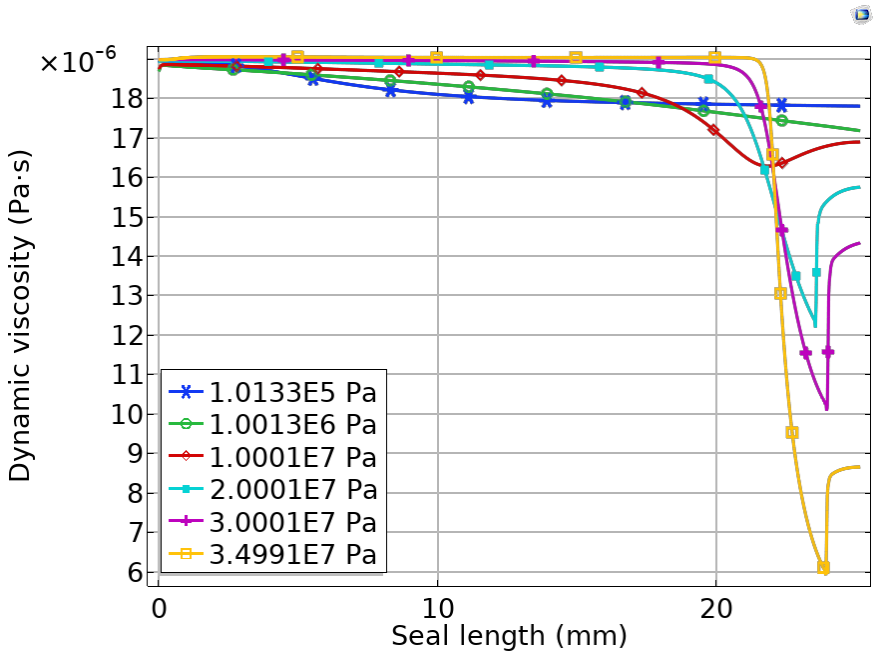

Figure 22: Dynamic Viscosity Data Collected from Bottom Boundary of the Seal

In this study, it is important to confirm the assumed limitation of the Reynold equation for this specific set of simulations. As assumed, there was highly compressible flow found near the exit of the clearance between the backing and the rotor. There was also highly compressible flow found in the clearance slightly past the throat of the seal. This can be seen in Figures 23 and 24.

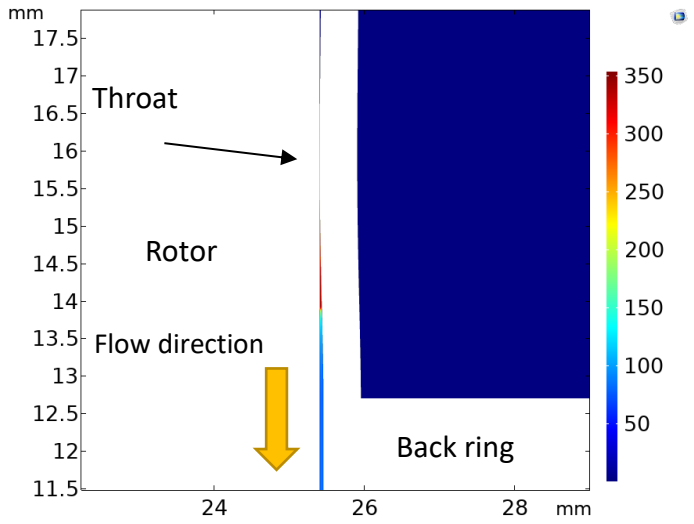

Figure 23: Highly Compressible Flow Downstream from the Throat, P_{in} = 35 MPa

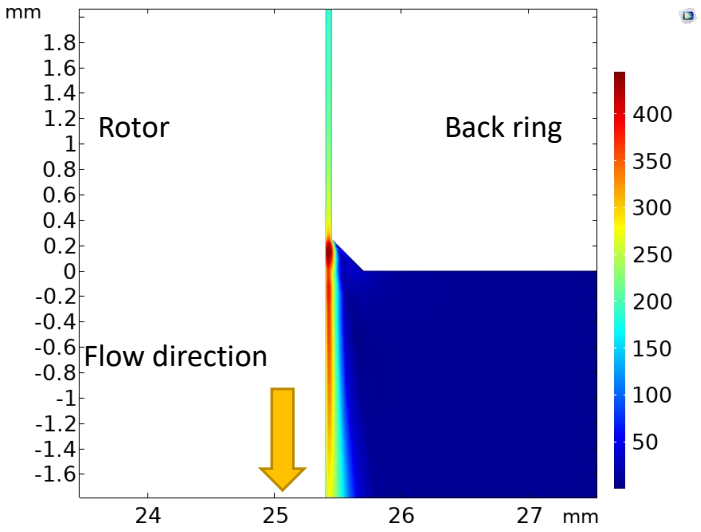

Figure 24: Highly Compressible Flow Near Exit by the Back Ring, P_{in} = 0.1 MPa

Lastly, the leakage rate of the seal must be analyzed and discussed. The leakage rate of the seal across its entire operational range can be seen in Figure 26. It was found that the leakage rate followed a quadratic trend with a peak when the input pressure, P_{in}, was 15 MPa. After that point, the leakage rate began to decline, dropping as low as $\dot{m}$ = 0.020 kg/s at P_{in} = 35 MPa. It is important to note that as inlet pressure increases, the deformation of the seal also increases. This, in turn, strengthens the throttling effect. This effect can be seen in Figure 21. In general, this figure shows similar characteristics to the pressure variations across a throttling value. The typical pressure variation across a throttling valve can be seen below in Figure 25.

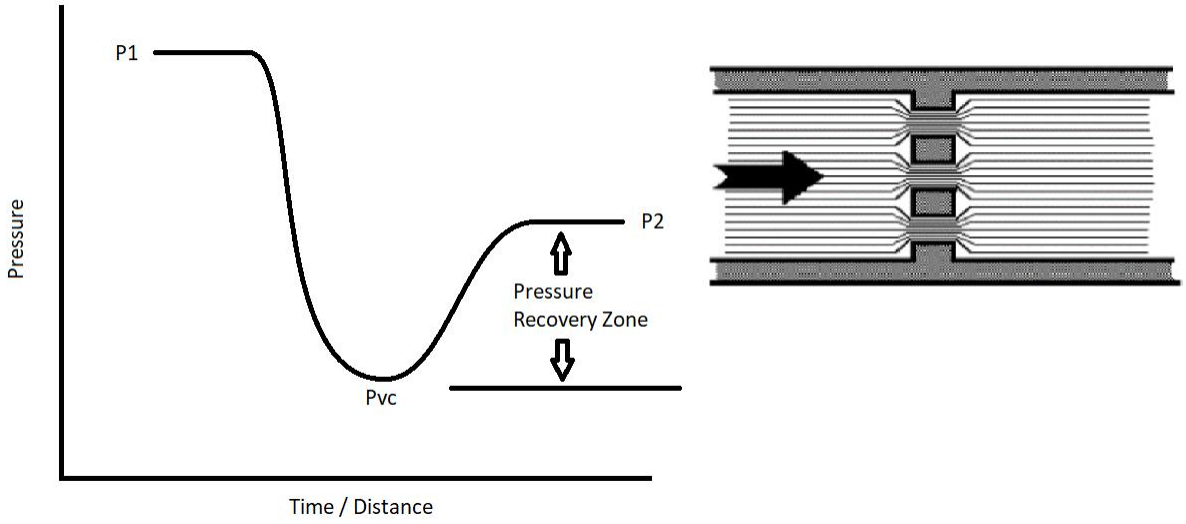

Figure 25: Typical Pressure Variation Across a Throttling Valve

The pressure value begins to decrease as the flow moves through the throat. Upon exiting the throat, the pressure increases in the pressure recover zone. As see in Figure 21, the recovery pressures begin to fade away as the inlet pressure increases.

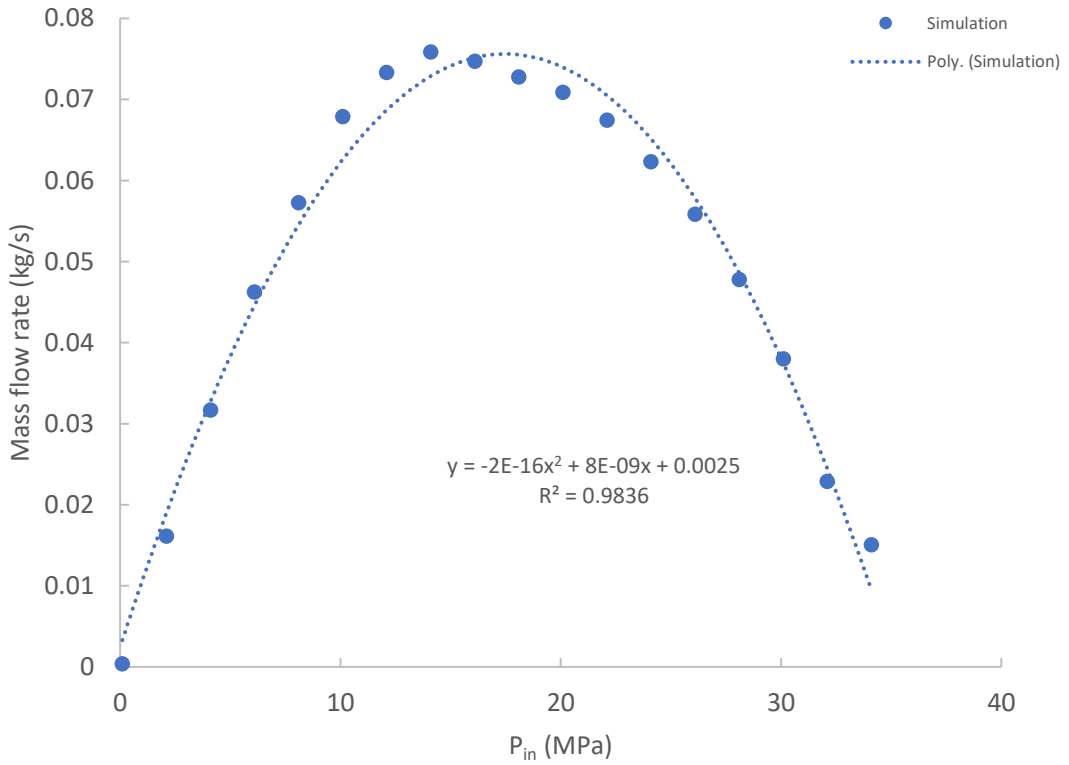

Figure 26: Leakage Rate of the Proposed EHD Seal from P_{in} = 0.1MPa to P_{in} = 35 MPa

This trend indicates that this seal and its current design geometry could be advantageous over traditional seal designs when the operating pressure is between 20 MPa to 30 MPa. It is important to note that the effects of surface roughness were not considered in this study. Incorporating the effects of surface roughness has the potential to further lower the leakage rate past the seal.

CHAPTER 5

CONCLUSION AND FUTURE WORK

The main conclusions of this study are listed below:

- The proof-of-concept seal analysis was successfully demonstrated for the proposed elastohydrodynamic (EHD) seal.
- The leakage rate obtained from the physics-based computer simulations followed a quadratic form with a peak at $\dot{m}$=0.075 kg/s at P_{in} = 15 MPa and then decaying to less than $\dot{m}$=0.040 kg/s at P_{in} = 30 MPa.
- The current seal geometry would operate best under pressure conditions ranging from 20 MPa to 30 MPa.
- The limitations of applying traditional analytical modeling techniques on this application were also confirmed due to the presence of highly compressible flow in the clearance of the seal.
- Overall, this design has the potential to offer a high pressure, low leakage, scalable sealing solution needed for the full realization of supercritical CO_2 power cycles and other turbomachinery.

For future work:

- An optimization study will be conducted to help determine optimum design parameters.
- A parametric analysis will also need to be performed to determine the impact of the design parameters. This includes changes to both material properties and seal geometry.
- Due to the small clearances required to make this seal function; a conjugate heat transfer analysis will need to be performed to account for thermal loads on the EHD seal.

- In the application of sCO_2 power cycles, real gas effects need to be considered as phase transitions could occur in the clearance of the seal.
- 3D simulations incorporating a rotating rotor will be conducted and a static test rig will be constructed and tested to evaluate the performance of the seal experimentally.

REFERENCES

Ahn, Yoonhan, Seong Jun Bae, Minseok Kim, Seong Kuk Cho, Seungjoon Baik, Jeong Ik Lee, and Jae Eun Cha. 2015. “Review of Supercritical CO2 Power Cycle Technology and Current Status of Research and Development.” *Nuclear Engineering and Technology* 47 (6): 647–61. https://doi.org/10.1016/J.NET.2015.06.009.

Bennett, Jeffrey A., A. Jasmin Melara, Lisa M. Colosi, and Andres F. Clarens. 2019. “Life Cycle Analysis of Power Cycle Configurations in Bioenergy with Carbon Capture and Storage.” *Procedia CIRP* 80: 340–45. https://doi.org/10.1016/j.procir.2018.12.014.

Benra, Friedrich Karl, Hans Josef Dohmen, Ji Pei, Sebastian Schuster, and Bo Wan. 2011. “A Comparison of One-Way and Two-Way Coupling Methods for Numerical Analysis of Fluid-Structure Interactions.” *Journal of Applied Mathematics* 2011. https://doi.org/10.1155/2011/853560.

Bidkar, Rahul A., Edip Sevincer, Jifeng Wang, Azam M. Thatte, Andrew Mann, Maxwell Peter, Grant Musgrove, Timothy Allison, and Jeffrey Moore. 2017. “Low-Leakage Shaft-End Seals for Utility-Scale Supercritical CO2 Turboexpanders.” *Journal of Engineering for Gas Turbines and Power* 139 (2): 1–8. https://doi.org/10.1115/1.4034258.

Chupp, Raymond E., Robert C. Hendricks, Scott B. Lattime, and Bruce M. Steinetz. 2006. “Sealing in Turbomachinery.” *Journal of Propulsion and Power* 22 (2): 313–49. https://doi.org/10.2514/1.17778.

Gong, Ru Zhi, De You Li, Hong Jie Wang, Lei Han, and Da Qing Qin. 2016. “Analytical Solution of Reynolds Equation under Dynamic Conditions.” *Proceedings of the Institution of Mechanical Engineers, Part J: Journal of Engineering Tribology* 230 (4): 416–27. https://doi.org/10.1177/1350650115604654.

Habchi, W., D. Eyheramendy, S. Bair, P. Vergne, and G. Morales-Espejel. 2008. “Thermal Elastohydrodynamic Lubrication of Point Contacts Using a Newtonian/Generalized Newtonian Lubricant.” *Tribology Letters* 30 (1): 41–52. https://doi.org/10.1007/s11249-008-9310-9.

Heshmat, Hooshang, Andrew Hunsberger, Zhaohui Ren, Said Jahanmir, and James F. Walton. 2013. “Oil-Free Bearings and Seals for Centrifugal Hydrogen Compressor.” *Tribology Online* 8 (1): 44–63. https://doi.org/10.2474/TROL.8.44.

Heshmat, Hooshang, James F. Walton II, and José Luis Córdova. 2018. “Technology Readiness of 5th and 6th Generation Compliant Foil Bearing for 10 MWE S-CO2 Turbomachinery Systems.” In *The 6th International Supercritical CO2 Power Cycles Symposium*, 1–29.

Hou, Guoqiang, Hua Su, Guoding Chen, and Yuhai Tian. 2020. “Performance Analysis of Compliant Cylindrical Intershaft Seal.” *Science Progress* 103 (3): 1–24. https://doi.org/10.1177/0036850420941957.

Kim, Min Seok, Seong Jun Bae, Seongmin Son, Bong Seong Oh, and Jeong Ik Lee. 2019. “Study of Critical Flow for Supercritical CO2 Seal.” *International Journal of Heat and Mass Transfer* 138 (August): 85–95. https://doi.org/10.1016/J.IJHEATMASSTRANSFER.2019.04.040.

Kulhánek, Martin, and Václav Dostál. 2011. “Supercritical Carbon Dioxide Cycles Thermodynamic Analysis and Comparison.” *Proceedings of SCCO2 Power Cycle Symposium*, 1–12.

Lugt, P. M., and G. E. Morales-Espejel. 2011. “A Review of Elasto-Hydrodynamic Lubrication Theory.” *Tribology Transactions* 54 (3): 470–96. https://doi.org/10.1080/10402004.2010.551804.

Pena de Souza Barros, Glycon, Carlos Barreira Martinez, Edna Maria de Faria Viana, Hélio Augusto Goulart Diniz, and Willian Moreira Duarte. 2019. “Labyrinth Seals - a Literature Review,” no. January. https://doi.org/10.26678/abcm.encit2018.cit18-0775.

Peterson, Wyatt, Thomas Russell, Farshid Sadeghi, and Michael Tekletsion Berhan. 2020. “A Strongly Coupled Finite Difference Method–Finite Element Method Model for Two-Dimensional Elastohydrodynamically Lubricated Contact.” *Journal of Tribology* 142 (5): 1–8. https://doi.org/10.1115/1.4045816.

Proestler, Stephan. 2002. “CFD Modeling of Brush Seals.” In *European CFX Conference*. https://www.researchgate.net/publication/292151012.

Rozova, Lyudmyla, and Gennadii Martynenko. 2020. “Information Technology in the Modeling of Dry Gas Seal for Centrifugal Compressors.” *CEUR Workshop Proceedings* 2608: 536–46.

Schowalter, David G., Nilanjana Basu, Ajey Walavalkar, and Richard R. Schultz. 2007. “On the Choice between Segregated and Coupled Solver Approaches When Using Computational Fluid Dynamics for Gas-Cooled Reactor Analysis.” *Nuclear Technology* 158 (1): 80–82. https://doi.org/10.13182/NT07-A3826.

Su, H., R. Rahmani, and H. Rahnejat. 2017. “Performance Evaluation of Bidirectional Dry Gas Seals with Special Groove Geometry.” *Tribology Transactions* 60 (1): 58–69. https://doi.org/10.1080/10402004.2016.1146380.

Wang, Xueliang, Meihong Liu, Sharon Kao-Walter, and Xiangping Hu. 2020. “Numerical Evaluation of Rotordynamic Coefficients for Compliant Foil Gas Seal.” *Applied Sciences (Switzerland)* 10 (11). https://doi.org/10.3390/app10113828.

White, Martin T., Giuseppe Bianchi, Lei Chai, Savvas A. Tassou, and Abdulnaser I. Sayma. 2021. “Review of Supercritical CO2 Technologies and Systems for Power Generation.” *Applied Thermal Engineering* 185 (November 2020). https://doi.org/10.1016/j.applthermaleng.2020.116447.

Wu, Tingcheng, and Luis San Andrés. 2019. “Gas Labyrinth Seals: On the Effect of Clearance and Operating Conditions on Wall Friction Factors – A CFD Investigation.” *Tribology International* 131 (October 2018): 363–76. https://doi.org/10.1016/j.triboint.2018.10.046.

Zhao, Hailin, Hua Su, and Guoding Chen. 2020. “Analysis of Total Leakage of Finger Seal with Side Leakage Flow.” *Tribology International* 150 (March): 106371. https://doi.org/10.1016/j.triboint.2020.106371.